

- Reese, D.E., Mikawa, T., Bader, D.M., 2002. Development of the coronary vessel system. *Circ. Res.* 91, 761–768.
- Saga, Y., Yagi, T., Ikawa, Y., Sakakura, T., Aizawa, S., 1992. Mice develop normally without tenascin. *Genes Dev.* 6, 1821–1831.
- Tamaoki, M., Imanaka-Yoshida, K., Yokoyama, K., Nishioka, T., Inada, H., Hiroe, M., Sakakura, T., Yoshida, T., 2005. Tenascin-C regulates recruitment of myofibroblasts during tissue repair after myocardial injury. *Am. J. Pathol.* 167, 71–80.
- Tanaka, K., Hiraiwa, N., Hashimoto, H., Yamazaki, Y., Kusakabe, M., 2004. Tenascin-C regulates angiogenesis in tumor through the regulation of vascular endothelial growth factor expression. *Int. J. Cancer* 108, 31–40.
- Tucker, R.P., Chiquet-Ehrismann, R., 2009. The regulation of tenascin expression by tissue microenvironments. *Biochim. Biophys. Acta* 1793, 888–892.
- Sugi, Y., Markwald, R.R., 1996. Formation and early morphogenesis of endocardial endothelial precursor cells and the role of endoderm. *Dev. Biol.* 175, 66–83.
- Van Den Akker, N.M.S., Lie-Venema, H., Maas, S., Eralp, I., DeRuiter, M.C., Poelmann, R.E., Gittenberger-De Groot, A.C., 2005. Platelet-derived growth factors in the developing avian heart and maturing coronary vasculature. *Dev. Dyn.* 233, 1579–1588.
- Waldo, K.L., Willner, W., Kirby, M.L., 1990. Origin of the proximal coronary artery stems and a review of ventricular vascularization in the chick embryo. *Am. J. Anat.* 188, 109–120.
- Verzi, M.P., McCulley, D.J., De Val, S., Dodou, E., Black, B.L., 2005. The right ventricle, outflow tract, and ventricular septum comprise a restricted expression domain within the secondary/anterior heart field. *Dev. Biol.* 287, 134–145.
- Vrancken Peeters, M.-P.F.M., Gittenberger-de Groot, A.C., Mentink, M.M.T., Hungerford, J.E., Little, C.D., Poelmann, R.E., 1997. The development of the coronary vessels and their differentiation into arteries and veins in the embryonic quail heart. *Dev. Dyn.* 208, 338–348.
- Zagzag, D., Shiff, B., Jallo, G.I., Greco, M.A., Blanco, C., Cohen, H., Hukin, J., Allen, J.C., Fridlander, D.R., 2002. Tenascin-C promotes microvascular cell migration and phosphorylation of focal adhesion kinase. *Cancer Res.* 62, 2660–2668.
- Zhang, H.Y., Kluge, M., Timpl, R., Chu, M.L., Ekblom, P., 2006. The extracellular matrix glycoproteins BM-90 and tenascin are expressed in the mesenchyme at sites of endothelial-mesenchymal conversion in the embryonic mouse heart. *Differentiation* 52, 211–220.

Role of Mesodermal FGF8 and FGF10 Overlaps in the Development of the Arterial Pole of the Heart and Pharyngeal Arch Arteries

Yusuke Watanabe, Sachiko Miyagawa-Tomita, Stéphane D. Vincent, Robert G. Kelly, Anne M. Moon, Margaret E. Buckingham

Rationale: The genes encoding fibroblast growth factor (FGF) 8 and 10 are expressed in the anterior part of the second heart field that constitutes a population of cardiac progenitor cells contributing to the arterial pole of the heart. Previous studies of hypomorphic and conditional *Fgf8* mutants show disrupted outflow tract (OFT) and right ventricle (RV) development, whereas *Fgf10* mutants do not have detectable OFT defects.

Objectives: Our aim was to investigate functional overlap between *Fgf8* and *Fgf10* during formation of the arterial pole.

Methods and Results: We generated mesodermal *Fgf8*; *Fgf10* compound mutants with *MesPICre*. The OFT/RV morphology in these mutants was affected with variable penetrance; however, the incidence of embryos with severely affected OFT/RV morphology was significantly increased in response to decreasing *Fgf8* and *Fgf10* gene dosage. *Fgf8* expression in the pharyngeal arch ectoderm is important for development of the pharyngeal arch arteries and their derivatives. We now show that *Fgf8* deletion in the mesoderm alone leads to pharyngeal arch artery phenotypes and that these vascular phenotypes are exacerbated by loss of *Fgf10* function in the mesodermal core of the arches.

Conclusions: These results show functional overlap of FGF8 and FGF10 signaling from second heart field mesoderm during development of the OFT/RV, and from pharyngeal arch mesoderm during pharyngeal arch artery formation, highlighting the sensitivity of these key aspects of cardiovascular development to FGF dosage. (*Circ Res.* 2010;106:495-503.)

Key Words: second heart field ■ arterial pole defects ■ pharyngeal arch artery defects

Malformations of the arterial pole of the heart account for more than 30% of human congenital heart defects.¹ Remodeling of the outflow tract (OFT) plays a critical role in the maturation of the arterial pole. As the heart matures, cushion tissue is formed in the OFT, as a result of an epithelial–mesenchymal transformation.² Rotation and shortening of the OFT are accompanied by fusion of the cushions to form a septum that divides the OFT into the aorta and pulmonary trunk. Subsequent morphogenetic events result in alignment of the aorta with the left ventricle and the pulmonary trunk with the right ventricle (RV).³ The OFT is derived from the anterior part of the second heart field (SHF), which in the mouse embryo, also contributes to the RV and ventricular septum.^{4–6} This field of splanchnic mesoderm initially lies medial to the cardiac crescent and then dorsally and anteriorly to the heart tube. In addition to myocardium, the SHF contributes smooth muscle to the base of the great arteries.^{6,7} A second source of cells, namely cardiac neural crest

(CNC), migrates from the neuroectoderm of the dorsal neural tube into the OFT and contributes to cushion formation and correct septation and alignment of the aortic and pulmonary outflows.^{8–10} CNC also interacts with the mesodermal cells of the SHF.¹¹ When CNC is ablated in the chick embryo, OFT elongation and looping of the cardiac tube is perturbed, leading to persistent truncus arteriosus and misalignment of the great arteries relative to the ventricles.¹⁰ Many signaling pathways in the SHF, CNC, and pharyngeal region control development of the arterial pole of the heart by affecting specification, proliferation, survival and differentiation of progenitor cells.¹²

SHF mesoderm also plays a role in the formation of the blood vessels that channel blood from the aorta and pulmonary trunk to the body and lungs. These arteries form within the third, fourth, and sixth pharyngeal arches, which are bilateral embryonic structures, consisting of surface ectoderm, inner endoderm, and a mesodermal core expressing SHF markers, that becomes surrounded by CNC. The endothelium of the pharyngeal arch

Original received May 26, 2009; revision received December 8, 2009; accepted December 10, 2009.

From the Department of Developmental Biology (Y.W., S.D.V., M.E.B.), Centre National de la Recherche Scientifique, Unité de Recherche Associée 2578, Institut Pasteur, Paris, France; Department of Pediatric Cardiology (S.M.-T.), Tokyo Women's Medical University, Tokyo, Japan; Developmental Biology Institute of Marseille-Luminy (R.G.K.), Unité Mixte de Recherche 6216 Université de la Méditerranée, Campus de Luminy, Marseille, France; and Departments of Pediatrics, Neurobiology, and Anatomy and Human Genetics (A.M.M.), University of Utah, Salt Lake City. Present address for Y.W.: Department of Developmental Neurobiology, Institute of Development, Aging and Cancer, Tohoku University, Sendai, Miyagi, Japan.

Correspondence to Margaret Buckingham, DPhil, Department of Developmental Biology, URA CNRS 2578, Institut Pasteur, 25 rue du Dr. Roux 75015 Paris, France. E-mail margaret.buckingham@pasteur.fr

© 2010 American Heart Association, Inc.

Circulation Research is available at <http://circres.ahajournals.org>

DOI: 10.1161/CIRCRESAHA.109.201665

Non-standard Abbreviations and Acronyms

CNC	cardiac neural crest
DORV	double outlet right ventricle
E	embryonic day
FGF	fibroblast growth factor
FGFR	fibroblast growth factor receptor
OFT	outflow tract
PAA	pharyngeal arch artery
RV	right ventricle
SHF	second heart field
VSD	ventricular septal defect

arteries (PAAs) is formed from the mesodermal core of the arches, whereas the vascular smooth muscle is predominantly CNC-derived.^{8,13,14} The PAAs form progressively following the anterior/posterior gradient of pharyngeal arch development, and from embryonic day (E)10.5 in the mouse embryo, remodeling leads to the mature PAA system. Many different cellular and genetic perturbations disrupt formation and/or remodeling of the PAAs.¹⁰

Fgf10 was identified as a gene expressed in cells that contribute to the OFT and RV in the mouse embryo, leading to the concept of the SHF.¹⁵ However *Fgf10*-null mutants have no evident SHF or PAA defects.¹⁶ *Fgf8* expression overlaps with that of *Fgf10* in the SHF from the cardiac crescent stage.¹⁵ Their expression is restricted to the anterior part of the SHF and is regulated by retinoic acid signaling on the anterior-posterior axis.¹⁷ *Fgf10* transcription extends from the anterior SHF into the mesodermal core of the pharyngeal arches, where *Fgf8* transcripts are difficult to detect. However, *Fgf8*^{LacZ/+}, *Fgf8*^{GFP/+}, and *Fgf8* enhancer-*LacZ* transgenic mice show LacZ or green fluorescent protein (GFP) expression in the anterior SHF and the mesodermal core of the arches, implying that *Fgf8* is transcribed there.^{18–20} Unlike *Fgf10*, *Fgf8* is also expressed in pharyngeal endoderm and ectoderm, where its expression is maintained, at least until E9.5.²¹ *Fgf8* mutants die at gastrulation²²; however, *Fgf8* hypomorphs survive to birth with variable OFT defects including persistent truncus arteriosus, transposition of the great arteries, and pharyngeal arch-related phenotypes. The fourth PAA is most severely affected resulting in interrupted or right aortic arch.^{23,24} Apoptosis of CNC was noted in these hypomorphs, suggesting fibroblast growth factor (FGF)8 signaling defects in surrounding tissues that directly or indirectly affect CNC, because *Fgf8* is not expressed in these cells. Subsequently, conditional mutagenesis of *Fgf8* with a battery of Cre recombinases, directed to pharyngeal ectoderm, pharyngeal endoderm, and SHF/pharyngeal arch mesoderm, has allowed tissue-specific phenotypes to be determined.^{13,19,20,25} Deletion of *Fgf8* in the pharyngeal ectoderm leads to CNC apoptosis, affecting PAA development.²⁵ The role of mesodermal FGF8 in PAA development has not been reported. Mesodermal and endodermal FGF8 are critical for OFT development, affecting the proliferation, survival, and transcriptional activity of SHF cells and their derivatives, in

addition to the function of the CNC. Deletion of *Fgf8* in early cardiogenic mesoderm with *MesP1Cre* causes initial OFT/RV hypoplasia and OFT alignment defects in survivors at incomplete penetrance.¹⁹ This implies that FGF10 may compensate for loss of FGF8 in the precardiac mesoderm.

In this study, we generated compound *Fgf8* and *Fgf10* mutants in the cardiac and pharyngeal mesoderm, using *MesP1Cre*. We show that PAA development is perturbed by mesodermal *Fgf8* deletion. The incidence and severity of PAA and of OFT defects increased with decreasing *Fgf8* and *Fgf10* gene dosage, resulting in severe defects in double *Fgf8*;*Fgf10* homozygous conditional mutants. These results reveal functional overlap of mesodermal FGF8 and FGF10 during SHF/OFT and PAA development, uncovering for the first time a role for FGF10 in the formation of the arterial pole of the heart. They also illustrate the sensitivity of these processes to incremental reductions in the level of FGF.

Methods

Mouse Lines

Mouse care and procedures were in accordance with institutional and national guidelines. The *Fgf8*-conditional mutant, *Fgf10* mutant, and *MesP1Cre* alleles are as previously described.^{19,26,27} The *MesP1^{Cre}* line was bred onto an *Fgf10*^{+/-} background and then onto *Fgf8*^{flax/+}, which was crossed with an *Fgf8*^{flax/flax};*Fgf10*^{+/-} line to obtain compound mutants. *Fgf8* and *Fgf10* genotyping by PCR was performed using the following primers: P1, P2, and 5'-GAGCTT-GCTGGGGGAAACTTCTGACTAGG-3' for *Fgf10*²⁶; and 5'-TGCCTAAGGGGAGAAGGCTGG-3', 5'-AAATTTAAGCTG-TGTAGATTCATAG-3', and 5'-GATTTCAGGAGAACAGACC-AGAG-3' primers for *Fgf8*. Numbers of embryos obtained at different stages are summarized in Online Table I (available in the Online Data Supplement at <http://circres.ahajournals.org>). Total numbers of embryos examined for each genotype at E10.5 and E15.5 to 18.5 are given in Tables 1 and 2, respectively.

Scoring OFT and RV Morphology

Right-sided views of the OFT and RV in embryos at E9.5 were scored according to four parameters, OFT length, the angle between the proximal and distal regions of the OFT, the size of the RV, and the extent of looping estimated by the angle of the OFT across the ventral body of the embryo. Scoring was performed by two independent observers blinded to genotype. There was remarkably little interobserver variability in the scores of individual embryos of all genotypes (not shown). Embryos were classified as normal, mild, moderate, and severe depending on the score (2 points for each parameter, with a maximum of 8 points: <2 points, severe; <4 points, moderate; <6 points, mild; ≥6, normal).

Histological Analysis and Ink Injection

Longitudinal sections (10 μm) were made in the OFT and pharyngeal arch region after paraffin embedding of E10.5 embryos. To visualize PAA formation, India ink was injected into the left ventricle or umbilical vein of E10.5 embryos using drawn glass pipettes.

Quantitative Real-Time PCR

The third to sixth pharyngeal arch region was dissected from embryos at 24 to 26 somite stages and stored in RNAlater (Qiagen) at -20°C until use. Total RNA was isolated from a pool of six samples for each genotype using RNeasy Mini Kit (Qiagen). The first strand cDNA was synthesized using SuperScript II Reverse Transcriptase (Invitrogen). Quantitative PCR was performed with Power SYBR Green PCR Master Mix (Applied Biosystems) with the StepOnePlus Real-Time PCR system (Applied Biosystems). Reverse transcription and quantitative PCR were repeated 3 times, and *Gapdh* was used to normalize gene expression. Primer sequences were 5'-TGAAAGCGGATACTTG-

Table 1. Incidence of Abnormal PAAs in *Fgf8;Fgf10* Compound Mutants With *MesP1Cre* at E10.5

<i>Fgf8;Fgf10</i> Genotype	No. of Embryos Examined	Second PAA			Third PAA			Fourth PAA			Sixth PAA			PAA Total	
		Normal	Presence		Normal	Absence		Normal	Absence		Normal	Absence		Normal	Abnormal
			Uni	Bi		Uni	Bi		Uni	Bi		Uni	Bi		
<i>flox/+;+/+</i>	10	10	0	0	10	0	0	10	0	0	8	0	2	8	2
<i>flox/+;+/-</i>	14	14	0	0	14	0	0	13	1	0	14	0	0	13	1
<i>flox/+;-/-</i>	3	3	0	0	3	0	0	3	0	0	3	0	0	3	0
<i>flox/flox;+/+</i>	16	15	0	1	11	4	1	12	4	0	15	0	1	8	8
<i>flox/flox;+/-</i>	13	11	2	0	8	5	0	8	5	0	13	0	0	6	7
<i>flox/flox;-/-</i>	7	4	1	2	4	2	1	1	4	2	7	0	0	0	7

PAAs examined after ink injection as shown in Figure 3. Unilateral (Uni) or bilateral (Bi) defects were scored as abnormal in all cases. χ^2 test was applied in comparisons of the following examples in the table. Second PAA: * $P < 0.05$, *Fgf8^{flox/flox}* vs *Fgf8^{flox/flox};Fgf10^{-/-}*; fourth PAA: ** $P < 0.01$, *Fgf8^{flox/flox}* vs *Fgf8^{flox/flox};Fgf10^{-/-}*; * $P < 0.05$, *Fgf8^{flox/flox};Fgf10^{+/-}* vs *Fgf8^{flox/flox};Fgf10^{-/-}*; PAA total: * $P < 0.05$, *Fgf8^{flox/flox}* vs *Fgf8^{flox/flox};Fgf10^{-/-}* and *Fgf8^{flox/flox};Fgf10^{+/-}* vs *Fgf8^{flox/flox};Fgf10^{-/-}*.

GAC-3' and 5'-TGTCGGGTACCTGAGCTTCT-3' for *Pea3*; 5'-GGACACAGATCTGGCTCACGA-3' and 5'-CGTGGCTACAGGACGACAAC-3' for *Erm*; *Isl1* primers were as designed by Liao et al.²⁸

Results

Fgf10 expression is observed in the anterior SHF and pharyngeal mesoderm, whereas *Fgf8* is expressed in pharyngeal endoderm and ectoderm in addition to these mesodermal tissues. To generate compound mutants for *Fgf8* and *Fgf10* in this mesoderm, we deleted the *Fgf8* conditional allele (*Fgf8^{flox}*) with *MesP1^{Cre/+}*. *Fgf10*-null homozygotes are not viable after birth, and we therefore used the *Fgf10* heterozygotes (*Fgf10^{+/-}*) for crosses (see Online Table I, *Fgf8^{flox/+};Fgf10^{+/-};MesP1^{Cre/+}* × *Fgf8^{flox/flox};Fgf10^{+/-}*). In the following text, *MesP1^{Cre/+}* is included in all genotypes.

OFT and RV Morphology Is Affected by Reducing *Fgf8* and *Fgf10* Dosage

In *Fgf8;Fgf10* double heterozygous (*Fgf8^{flox/+};Fgf10^{+/-}*) (Figure 1B) and *Fgf8^{flox/+};Fgf10^{-/-}* embryos (Figure 1C), OFT and RV morphology is normal at E9.5, similar to that of *Fgf8^{flox/+}* embryos (Figure 1A). *Fgf8^{flox/flox}* embryos have hypomorphic OFTs and RVs (Figure 1D through 1F), as previously reported with a *MesP1Cre* at E9.5.¹⁹ When *Fgf10* dosage was decreased in addition to *Fgf8* deletion (Figure 1G through 1L), more severe phenotypes were observed, includ-

ing hypoplasia of the second and third pharyngeal arches (Figure 1I and 1L). This was also illustrated by sections of the OFT at E10.5 showing normal presence of CNC and initiation of epithelial-mesenchymal transition before cushion formation in control *Fgf8;Fgf10* double heterozygotes (Figure 1M). In contrast, CNC invasion and epithelial-mesenchymal transition were notably compromised in *Fgf8;Fgf10* double homozygous mutants (Figure 1O) and already affected in *Fgf8^{flox/flox}* mutants (Figure 1N).

To confirm and quantify this, we scored OFT and RV morphology on the basis of OFT length, the angle between the proximal and distal regions of the OFT, RV size and extent of looping, by a blind test. Phenotypes were classified as normal, mild, moderate, and severe, depending on the score (Figure 2A). The number of abnormal *Fgf8^{flox/flox}* embryos was less than in our previous report, probably because in that case the *Fgf8^{flox/+}* cross was analyzed.¹⁹ The important point, shown in Figure 2A, is that increasingly affected embryos were observed as *Fgf8* dosage is reduced. No severe phenotypes were observed with *Fgf8* deletion alone, whereas no normal hearts were observed in *Fgf8;Fgf10* double homozygous mutants. This result shows that FGF10 functions with FGF8 in OFT and RV development. To verify that FGF signaling was attenuated in *Fgf8;Fgf10* double homozygous mutants, we performed quantitative PCR analysis for FGF target genes, *Pea3* and *Erm*, using RNA isolated from the pharyngeal region (including SHF mesoderm, endoderm,

Table 2. Incidence of Abnormal Heart and PAAs in *Fgf8;Fgf10* Compound Mutants With *MesP1Cre* at E15.5 to E18.5

<i>Fgf8;Fgf10</i> Genotype	No. of Embryos Examined	Heart			Pharyngeal Arch Arteries				
		Normal	TGA/DORV	VSD	Normal	Short or Absent LCC	ARSA	RtAA	Narrow AoA
<i>flox/+;+/+</i>	7	7	0	0	7	0	0	0	0
<i>flox/+;+/-</i>	13	13	0	0	13	0	0	0	0
<i>flox/+;-/-</i>	4	4	0	0	4	0	0	0	0
<i>flox/flox;+/+</i>	11	9	1	2	8	2	1	1	0
<i>flox/flox;+/-</i>	13	8	1	5	9	2	2	1	1
<i>flox/flox;-/-</i>	5	1	1	3	1	2	2	0	1

One or more arterial pole or PAA malformations were scored as abnormal in all cases. χ^2 test was applied in comparisons of the following examples in the table. Heart: * $P = 0.018$, *Fgf8^{flox/flox}* vs *Fgf8^{flox/flox};Fgf10^{-/-}*; PAAs: * $P = 0.049$, *Fgf8^{flox/flox}* vs *Fgf8^{flox/flox};Fgf10^{-/-}*. AoA indicates aortic arch; ARSA, aberrant origin of right subclavian artery; RtAA, right aortic arch; TGA, transposition of the great arteries.

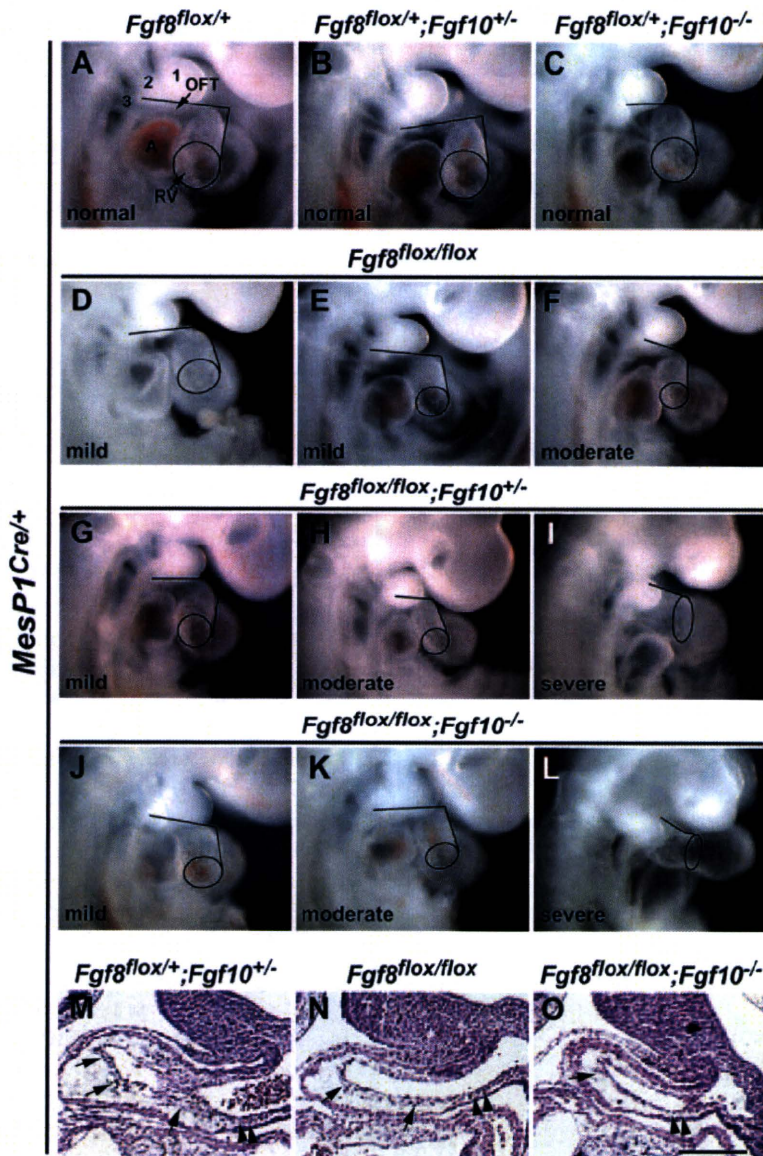


Figure 1. OFT and RV morphology of E9.5 *Fgf8;Fgf10;MesP1Cre* compound mutants. A through L, Right lateral views of embryos are shown, and genotypes are listed above the images. In *Fgf8^{flox/+}* (A), *Fgf8^{flox/+};Fgf10^{+/-}* (B), and *Fgf8^{flox/+};Fgf10^{-/-}* (C) embryos, OFT and RV morphology is normal. In *Fgf8^{flox/flox}* (D through F), *Fgf8^{flox/flox};Fgf10^{+/-}* (G through I), and *Fgf8^{flox/flox};Fgf10^{-/-}* (J through L) embryos, the angle between the proximal and distal regions of the OFT is more obtuse (lines) or, in severe cases, absent, and/or the RV is smaller (circle) when compared with normal hearts (A through C). M through O, Sections of the OFT of E10.5 embryos with the genotypes indicated. CNC has invaded the OFT (arrowheads), and the endothelium is beginning to undergo epithelial-mesenchymal transformation³¹ (arrows), where the cushions will form in *Fgf8;Fgf10* double heterozygous control embryos (M). In *Fgf8;Fgf10* mutant embryos, these processes are compromised (N and O) and most notably in the double homozygous mutant, the OFT is smaller and misshapen (O). Pharyngeal arches are numbered in A. Scale bar=200 μ m.

and ectoderm) of compound mutant embryos (Figure 2B). We could not detect differences between *Fgf8^{flox/+};Fgf10^{+/-}* and *Fgf8^{flox/flox};Fgf10^{+/-}* mutants, suggesting that FGF8 in pharyngeal endoderm and ectoderm, together with FGF10 from 1 allele of *Fgf10* expressed in mesoderm, lead to levels of *Pea3* and *Erm* transcription in the pharyngeal region that obscure the reduction in the mesoderm. However, significant downregulation of the signaling read out from all FGF sources was detected in *Fgf8;Fgf10* double homozygous mutants (Figure 2B). These results demonstrate the effect on FGF signaling readout of removing both alleles of *Fgf10* on an *Fgf8* mesodermal-null background. Transcripts for *Isl1*, a key transcription factor required in the SHF,²⁹ were also downregulated in the double homozygous mutants (Figure 2B). Apoptosis and proliferation were altered in *Isl1*-positive SHF cells in the double homozygous mutants (Online Figure I, A through D), as reported for *Fgf8^{flox/-}* mutants,¹⁹ thus explaining the reduction in *Isl1* transcripts.

Mesodermal FGF8 and FGF10 Regulate Development of the PAAs

PAAs, visualized by ink injection, were examined in *Fgf8;Fgf10* compound mutants at E10.5 (Figure 3). At this stage, normal mouse embryos have third, fourth, and sixth bilateral PAAs (Figure 3A through 3C). PAA development was affected in some *Fgf8^{flox/flox}* embryos (Figure 3D through 3F and 3M). Ectodermal *Fgf8* ablation causes bilateral fourth PAA hypoplasia or aplasia.²⁵ With mesodermal deletion of *Fgf8*, we observed not only fourth PAA defects but also effects on the development of the third and sixth PAAs and abnormal maintenance of the second PAA (Figure 3M). *Fgf10^{-/-}* mutants did not show any PAA defects, as reported previously (data not shown).³⁰ However, deletion of one allele of *Fgf10* increased the proportion of PAA defects in *Fgf8^{flox/flox}* embryos (Figure 3G through 3I and 3M), and this incidence was further increased in *Fgf8;Fgf10* double homozygous mutants (Figure 3J through 3M). Apoptosis in CNC was observed at the level of the developing fourth PAA,

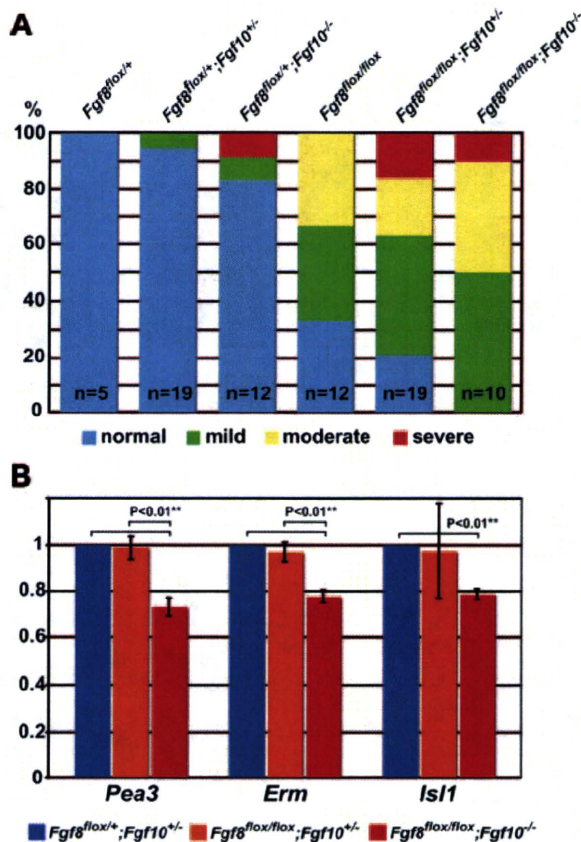


Figure 2. Reduction of FGF dosage affects morphology and gene expression in the OFT and RV. A, Phenotype of OFT and RV morphology of E9.5 *Fgf8;Fgf10;MesP1Cre* compound mutants are divided into normal, mild, moderate, and severe according to OFT length, the angle between the proximal and distal regions of the OFT, RV size, and looping, based on blind tests. Increasingly severe phenotypes (see Figure 1) are observed as *Fgf* gene dosage is reduced. Numbers of embryos (n) are indicated below each column. B, Quantitative PCR analysis of transcripts for FGF signaling effectors, *Pea3* and *Erm*, and for *Isl1*, normalized to *Gapdh* transcripts, in extracts from the pharyngeal region dissected from 6 embryos, with the genotypes indicated, at 24 to 26 somite stages. Results are shown relative to that for *Fgf8;Fgf10* double heterozygotes. Error bar indicates the SD.

in *Fgf8^{flx/flx};Fgf10^{+/-}* mutants (Online Figure I, E and F), as reported for *Fgf8* hypomorphic, *Fgf8^{flx/-};AP2alresCre*, and *Fgf8^{flx/-};Hoxa3Cre* mutants.^{23,25} Sections also illustrated the severe PAA defects seen in *Fgf8;Fgf10* double homozygous mutants (Figure 3O), compared to control *Fgf8;Fgf10* double heterozygous embryos (Figure 3N). These results, summarized in Table 1, show that mesodermal FGF8 and FGF10 are critical for PAA development.

Heart and PAA Phenotypes at Later Developmental Stages Are Consistent With Those Observed Earlier

The adult configuration of the heart and great vessels is largely established by E15.5: the ventricles are separated by the ventricular septum; the OFT has given rise to myocardium at the base of the aorta and pulmonary trunk; and the third, fourth, and sixth PAAs have been remodeled into the common carotid and subclavian arteries and contributed to part of the

aortic arch and ductus arteriosus (Figure 4A and 4B). In the heart of *Fgf8^{flx/flx}* embryos, as previously reported,¹⁹ transposition of the great arteries, double outlet right ventricle (DORV), and ventricular septal defects (VSDs) were observed, although in a minority of cases (Figure 4F and 4G; Table 2). In *Fgf8^{flx/flx};Fgf10* compound mutants, these heart defects became more frequent as *Fgf10* dosage is reduced (Figure 4J, 4L, and 4M; Table 2). Defects in PAA derivatives reflect the PAA abnormalities seen in mutants at E10.5. We observed absence of the left common carotid artery (Figure 4E, 4H, and 4K), which was attributable to loss of the left third PAA; aberrant origin of the right subclavian artery (Figure 4F, 4I, and 4K), which is attributable to loss of the right fourth PAA; right aortic arch (Figure 4I), which is caused by loss of the left fourth PAA (the aortic arch is probably replaced by the right fourth PAA); and narrow aortic arch (Figure 4L), because of a hypoplastic left fourth PAA. Consistent with earlier defects of the heart and PAA, the incidence of these later defects in surviving embryos was significantly increased when *Fgf10* gene dosage was reduced, in conjunction with mesodermal deletion of *Fgf8* (Table 2). These results confirm the functional overlap of mesodermal FGF8 and FGF10 in the development of the arterial pole of the heart and PAA, seen at earlier stages.

Discussion

The phenotypic analysis that we present establishes a role for FGF10 as well as FGF8 in the formation of the arterial pole of the heart and demonstrates that this process is highly sensitive to FGF dosage. Furthermore, we show that the level of FGF8 and FGF10 signaling is not only critical for OFT development, but also for the PAAs and their derivatives. Unexpectedly, mesodermal, as well as ectodermal,²⁵ expression of *Fgf8* is important for the correct formation of these arteries and thus for cardiac function.

Most of the mutant embryos survive to late fetal stages, permitting analysis of the definitive morphology of the arterial pole. This is in contrast to previously reported observations on *Fgf8^{flx/-};MesP1^{Cre/+}* embryos of which 65% died by E10.5.¹⁹ This difference probably reflects the mesodermal specificity of deletion of the floxed alleles, which in our case (*Fgf8^{flx/flx};MesP1^{Cre/+}*) are entirely responsible for generating the mutant phenotype. At early stages, in *Fgf8* and in *Fgf8;Fgf10* mutants, we observe hypoplasia of both the OFT and RV, which also derives from SHF cells expressing *Fgf8*,^{15,20} as well as *Fgf10*.¹⁵ This reflects apoptosis and loss of proliferation of progenitor cells, observed when FGF signaling is abrogated, attributable either to mutation of mesodermal *Fgf8* and *Fgf10* (in this study)¹⁹ or to interference with FGF signal reception in the SHF.^{31,32} A reduction in SHF cells is also indicated by a decrease in *Isl1* expression, reported for the more severe *Fgf8^{flx/-};MesP1^{Cre}* phenotype¹⁹ and notable in *Fgf8^{flx/flx};Fgf10^{-/-}* double mutants. As the OFT matures, leading to epithelial-mesenchymal transition, cushion formation is initiated and CNC migrates into the OFT. These processes are affected when FGF signaling in mesoderm is abrogated,^{31,32} and the phenotypes again are striking in the *Fgf8^{flx/flx};Fgf10^{-/-}* double mutants. The effects of FGF signaling from the SHF on CNC are indirect, because the arterial pole of the heart develops normally when FGF signaling

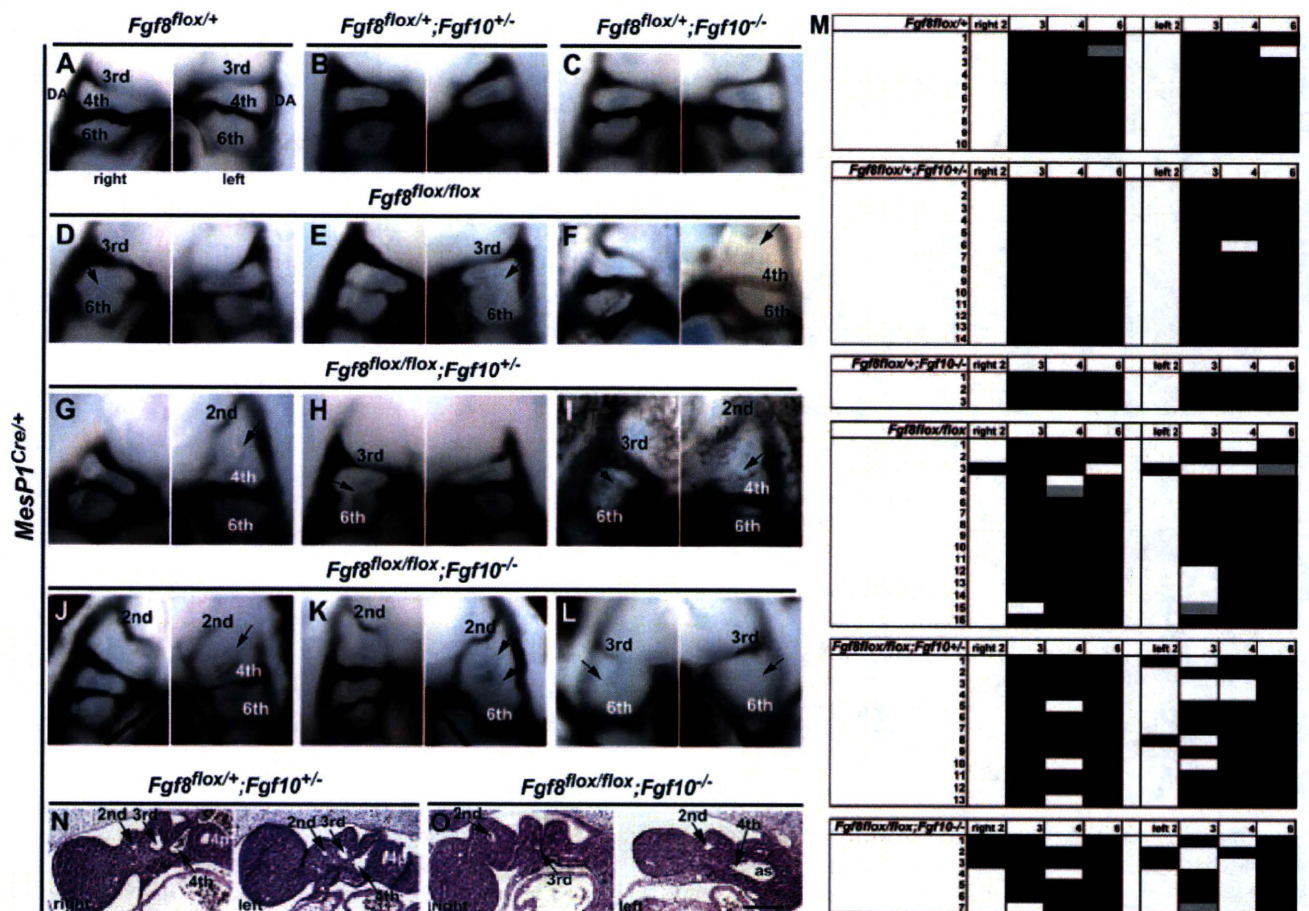


Figure 3. PAAs in *Fgf8;Fgf10;MesP1Cre* compound mutants. A through L, PAAs are visualized by ink injection at E10.5. Genotypes are listed above the images. At E10.5, third, fourth, and sixth PAAs are observed in the arches on both sides of the embryo. *Fgf8^{flax/+}*, *Fgf8^{flax/+};Fgf10^{+/-}*, and *Fgf8^{flax/+};Fgf10^{-/-}* embryos have normal PAA patterns (A through C), whereas *Fgf8^{flax/flax}*, *Fgf8^{flax/flax};Fgf10^{+/-}* and *Fgf8^{flax/flax};Fgf10^{-/-}* embryos have various defects (arrows in D through L), including missing third, fourth, and sixth PAAs, and retention of the second PAA. M, Summary of ink injection results for each embryo examined. Black columns represent PAAs labeled by the ink; white columns, PAAs where ink labeling was negative; gray columns, PAAs that were weakly labeled. N and O, Sections of embryos at E10.0 in the region of the pharyngeal arches, with the genotypes indicated. In control *Fgf8;Fgf10* double heterozygous embryos, the second, third, and fourth arches are evident (N, arrows). The fourth pharyngeal pouch (4p) is also visible. In the *Fgf8;Fgf10* double homozygous mutant sections shown, the fourth arch is present but the PAA is not detectable on the right-hand side. On the left side, the third PAA is missing (O). as indicates aortic sac; DA, dorsal aorta. Scale bar=200 μ m.

in CNC is diminished.^{31,32} We propose that the Bmp/TGF β pathway mediates the action of mesodermal FGF signaling on CNC, because components of this pathway are downregulated in *Fgf8* mutants.³¹ This would also have effects on the Nkx2.5 transcriptional network in the SHF.³³ Further identification of targets of Pea3/Erm, transcriptional effectors of FGF signaling, should provide more insight into the FGF regulatory network. Failure of CNC migration into the OFT probably results from abnormal cell death in the pharyngeal arches.^{20,23–25} Upregulation of FGF signaling, observed with CNC ablation³⁴ or in *Tbx3* mutants,³⁵ also disrupts OFT development, demonstrating a critical requirement for precise levels of FGF signaling during arterial pole formation. Because CNC contributes the smooth muscle of the nascent PAAs and their mature derivatives, CNC death in *Fgf8;Fgf10;MesP1Cre* compound mutants contributes to defects in the stabilization and remodeling of these arteries. In *Fgf8^{flax/+}; AP2 α resCre* mutants where *Fgf8* was deleted in pharyngeal ectoderm, major defects in the fourth PAA were documented, with minor effects on third and sixth PAAs.²⁵ *Fgf8*

deletion in the mesodermal core of the arches causes similar effects on third, fourth and sixth PAAs. The increase in PAA defects in *Fgf8^{flax/flax};Fgf10^{-/-}* double mutants reveals an unsuspected role for FGF10 in PAA development. We also observe some cases of second PAA persistence at E10.5, probably reflecting a developmental delay. Mesodermal FGF signaling is clearly also necessary and the timing of this requirement may precede the appearance of CNC. *MesP1Cre* is activated at about E6.5, well before somites begin to form, whereas the *Mef2c* regulatory element that drives *Mef2cCre* expression in the SHF, including pharyngeal arch mesoderm, is activated later, from 2 to 3 somite stages.¹⁹ Because PAA formation and remodeling are normal in *Fgf8^{flax/+}; Mef2cCre* embryos (16/16; A.M.M., unpublished data, 2005) the *MesP1Cre* phenotypes indicate that mesodermal FGF signaling is required at early stages to support PAA development, before CNC arrive in the arches.

Cardiac defects in surviving *Fgf8;Fgf10* mutants, present as alignment defects of the aorta and pulmonary trunk (transposition of the great arteries) together with DORV and

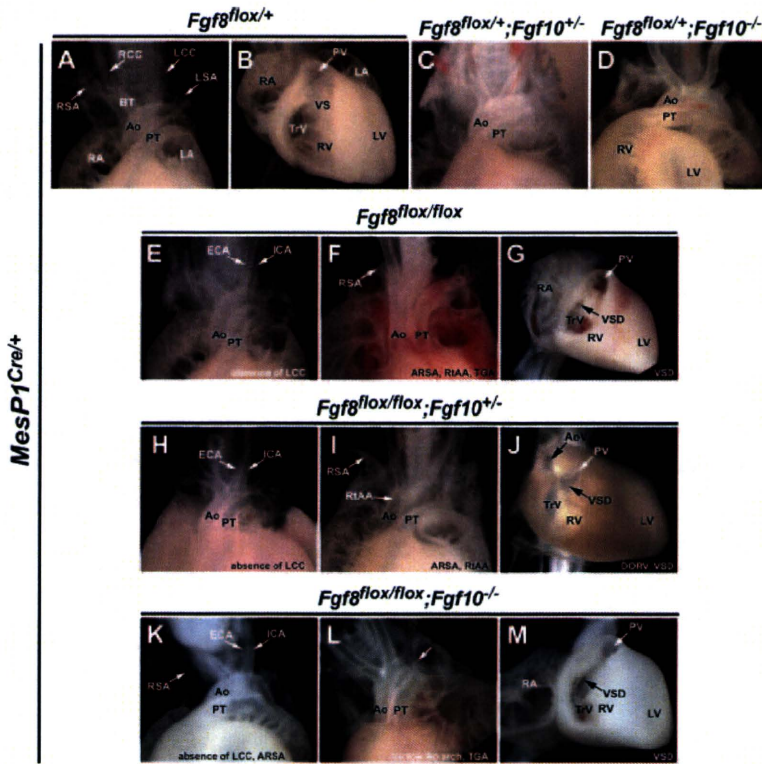


Figure 4. Heart and PAA defects in *Fgf8;Fgf10; MesP1Cre* compound mutants at later stages (E15.5 to E18.5). Genotypes are listed above the images. A through C, Heart and PAAs have normal structures in *Fgf8^{flox/+}* and *Fgf8^{flox/+};Fgf10^{+/-}* embryos. In *Fgf8^{flox/+};Fgf10^{-/-}* and *Fgf8^{flox/flox};Fgf10^{-/-}* embryos (D and K through M), in the absence of FGF10, the position of the apex of the heart is random, and the pulmonary arteries are absent; other parts of the *Fgf8^{flox/+};Fgf10^{-/-}* heart and the PAAs are normal (D). E through M, *Fgf8^{flox/flox}* (E through G), *Fgf8^{flox/flox};Fgf10^{+/-}* (H through J), and *Fgf8^{flox/flox};Fgf10^{-/-}* (K through M) embryos have PAA and heart defects. As examples of PAA defects, E, H, and K show external and internal carotid arteries (ECA and ICA) directly arising from the aortic arch, F, I, and K show an aberrant origin of the right subclavian artery (ARSA), and an abnormal right aortic arch (RtAA) is also observed (I). Heart defects include abnormal alignment of the OFT (transposition of the great arteries [TGA]; DORV) (F, J, and L) and VSDs (G, J, and M). Ao indicates aorta; AoV, aortic valve; BT, brachiocephalic trunk; LA, left atrium; LCC, left common carotid artery; LSA, left subclavian artery; LV, left ventricle; PT, pulmonary trunk; PV, pulmonary valve; RA, right atrium; RCC, right common carotid artery; RSA, right subclavian artery; TrV, tricuspid valve; VS, ventricular septum.

VSDs, reflecting earlier malpositioning of the OFT and affected CNC. These defects also predominate when mesodermal *Fgf8* is mutated (Table 2), whereas persistent truncus arteriosus is seen when *Fgf8* is deleted in both mesoderm and pharyngeal endoderm.^{13,19} The defects that we observe later in carotid and subclavian arteries and in the aortic arch reflect earlier defects in PAA development. When *Fgf8* is deleted in pharyngeal ectoderm,²⁵ the range and frequency of defects is different from those observed with mesodermal deletion of *Fgf8*, or when *Fgf10* is also mutated. In addition to dose dependence, this result reveals the importance of paracrine effects of FGF signaling during PAA development.

Deletion of *Fgf8* and *Fgf10* does not result in total loss of the structures that depend on FGF signaling. This may be because other signaling pathways, such as *Bmp/TGFβ*, which lies downstream of FGF8,¹⁹ also function independently to promote formation of the arterial pole of the heart and the PAAs. It may also reflect the ability of other FGFs to compensate in the SHF and pharyngeal arches. *Fgf15*, for example, is expressed in pharyngeal mesoderm and *Fgf15* mutants have cardiac defects (DORV, overriding aorta and VSD), suggesting that FGF15 may play a role in the development of the arterial pole of the heart.³⁶ Loss of *Fgf3*, which is also expressed in pharyngeal endoderm, does not cause heart or PAA phenotypes, but *Fgf3^{-/-};Tbx1^{+/-}* mutants have an aberrant origin of the right subclavian artery and interrupted aortic arch.³⁷

In considering the relative roles of FGF8 and FGF10, the former is more widely produced, by pharyngeal endoderm and pharyngeal ectoderm, as well as by mesoderm in the anterior SHF and in its extension into the core of the pharyngeal arches, whereas FGF10 production is predominantly limited to the mesoderm. Both FGFs bind to FGF receptor (FGFR)2, although

FGF10 binds preferentially to the IIIb isoform, whereas FGF8 binds to IIIc and also has affinity for FGFR1, FGFR3IIIc, and FGFR4.^{38–40} Mutational analysis of *Fgfr1* and *Fgfr2* suggests that FGFR1 is the dominant receptor in the SHF,³¹ although FGFR2 is also active and indeed in a different genetic background may be more important.³² Mutation of *Fgfr1* and *Fgfr2* in mesoderm compromises OFT development, as does overexpression of *Sprouty2*, an inhibitor of intracellular FGF signaling.³¹ Examination of *Fgfr2-IIIb* mutants shows later cardiac defects,¹⁶ but no striking effects on the early OFT, although RV hypoplasia, overriding aorta, DORV, and VSDs were noted. The question of in vivo FGF/receptor specificity is complex and the only clear conclusion to date is that FGFR1 and FGFR2 are required for FGF8 and FGF10 signaling, playing an essential role in the control of SHF progenitor cell proliferation and downstream signaling cascades³¹ during OFT morphogenesis.

The *Tbx1* mutant phenotype, which recapitulates cardiovascular aspects of human DiGeorge syndrome,^{41–43} overlaps with that of *Fgf8* hypomorphs.^{23,24} *Tbx1* is expressed in the mesoderm of the anterior SHF, including the mesodermal core, endoderm, and ectoderm of the pharyngeal arches,^{44,45} like *Fgf8*. Genetic analysis suggests that *Tbx1* lies upstream of *Fgf8* in pharyngeal endoderm⁴⁶ and also affects *Fgf8* and *Fgf10* expression in SHF mesoderm.^{18,46,47} Phenotypic analysis of embryos after tissue specific deletion of *Tbx1* with mesodermal *Cre* lines has shown that mesodermal *Tbx1* is critical for SHF and OFT development.⁴⁸ This is similar to FGF8¹⁹ and to FGF10 as we now show.

Our findings demonstrate for the first time that mesodermal FGF10, as well as FGF8, is important for formation of the arterial pole of the heart and the PAAs, providing new insight into the cardiovascular abnormalities seen in Di-

George syndrome. Furthermore, mutations in *Fgf10* and *Fgf8* that affect their expression in pharyngeal mesoderm may underlie human congenital heart and vascular defects.

Acknowledgments

We thank Y. Saga for the *MesP1*^{Cre/+} line and N. Itoh and S. Kato for *Fgf10*^{+/-} mice. We thank C. Bodin and C. Cimper for help with histology, E. Pecnard and S. Coqueran for genotyping, E.J. Park for scoring of OFT/RV morphology of embryos, and to members of our laboratory and S. Zaffran for helpful discussions.

Sources of Funding

The work performed in the laboratory of M.E.B. was supported by the Institut Pasteur and the Centre National de la Recherche Scientifique, with grants from the European Union Integrated Project "Heart Repair" LHSM-CT2005-018630 (also to R.G.K.) and the CardioCell LT2009-223372 project. The work performed in the laboratory of A.M.M. was supported by the National Institute of Child Health and Development. Y.W. received a fellowship from the European Union Integrated Project "Heart Repair." S.M.-T. received a fellowship from the Naito Foundation to perform work for 6 months in the laboratory of M.E.B.

Disclosures

None.

References

- Lloyd-Jones D, Adams R, Carnethon M, De Simone G, Ferguson TB, Flegal K, Ford E, Furie K, Go A, Greenland K, Haase N, Hailpern S, Ho M, Howard V, Kissela B, Kittner S, Lackland D, Lisabeth L, Marelli A, McDermott M, Meigs J, Mozaffarian D, Nichol G, O'Donnell C, Roger V, Rosamond W, Sacco R, Sorlie P, Stafford R, Steinberger J, Thom T, Wasserthiel-Smoller S, Wong N, Wylie-Rosett J, Hong Y. Heart disease and stroke statistics—2009 update: a report from the American Heart Association Statistics Committee and Stroke Statistics Subcommittee. *Circulation*. 2009;119:e21–e181.
- Nakajima Y, Yamagishi T, Hokari S, Nakamura H. Mechanisms involved in valvuloseptal endocardial cushion formation in early cardiogenesis: roles of transforming growth factor (TGF)-beta and bone morphogenetic protein (BMP). *Anat Rec*. 2000;258:119–127.
- Webb S, Qayyum SR, Anderson RH, Lamers WH, Richardson MK. Septation and separation within the outflow tract of the developing heart. *J Anat*. 2003;202:327–342.
- Buckingham M, Meilhac S, Zaffran S. Building the mammalian heart from two sources of myocardial cells. *Nat Rev Genet*. 2005;6:826–835.
- Franco D, Meilhac SM, Christoffels VM, Kispert A, Buckingham M, Kelly RG. Left and right ventricular contributions to the formation of the interventricular septum in the mouse heart. *Dev Biol*. 2006;294:366–375.
- Verzi MP, McCulley DJ, De Val S, Dodou E, Black BL. The right ventricle, outflow tract, and ventricular septum comprise a restricted expression domain within the secondary/anterior heart field. *Dev Biol*. 2005;287:134–145.
- Waldo KL, Hutson MR, Ward CC, Zdanowicz M, Stadt HA, Kumiski D, Abu-Issa R, Kirby ML. Secondary heart field contributes myocardium and smooth muscle to the arterial pole of the developing heart. *Dev Biol*. 2005;281:78–90.
- Jiang X, Rowitch DH, Soriano P, McMahon AP, Sucov HM. Fate of the mammalian cardiac neural crest. *Development*. 2000;127:1607–1616.
- Nakamura T, Colbert MC, Robbins J. Neural crest cells retain multipotential characteristics in the developing valves and label the cardiac conduction system. *Circ Res*. 2006;98:1547–1554.
- Hutson MR, Kirby ML. Model systems for the study of heart development and disease. Cardiac neural crest and conotruncal malformations. *Semin Cell Dev Biol*. 2007;18:101–110.
- Waldo KL, Hutson MR, Stadt HA, Zdanowicz M, Zdanowicz J, Kirby ML. Cardiac neural crest is necessary for normal addition of the myocardium to the arterial pole from the secondary heart field. *Dev Biol*. 2005;281:66–77.
- Rochais F, Mesbah K, Kelly RG. Signaling pathways controlling second heart field development. *Circ Res*. 2009;104:933–942.
- Brown CB, Wenning JM, Lu MM, Epstein DJ, Meyers EN, Epstein JA. Cre-mediated excision of *Fgf8* in the *Tbx1* expression domain reveals a critical role for *Fgf8* in cardiovascular development in the mouse. *Dev Biol*. 2004;267:190–202.
- Engleka KA, Gitler AD, Zhang M, Zhou DD, High FA, Epstein JA. Insertion of Cre into the *Pax3* locus creates a new allele of *Splotch* and identifies unexpected *Pax3* derivatives. *Dev Biol*. 2005;280:396–406.
- Kelly RG, Brown NA, Buckingham ME. The arterial pole of the mouse heart forms from *Fgf10*-expressing cells in pharyngeal mesoderm. *Dev Cell*. 2001;1:435–440.
- Marguerie A, Bajolle F, Zaffran S, Brown NA, Dickson C, Buckingham ME, Kelly RG. Congenital heart defects in *Fgfr2-IIIb* and *Fgf10* mutant mice. *Cardiovasc Res*. 2006;71:50–60.
- Ryckebusch L, Wang Z, Bertrand N, Lin SC, Chi X, Schwartz R, Zaffran S, Niederreither K. Retinoic acid deficiency alters second heart field formation. *Proc Natl Acad Sci U S A*. 2008;105:2913–2918.
- Hu T, Yamagishi H, Maeda J, McAnally J, Yamagishi C, Srivastava D. *Tbx1* regulates fibroblast growth factors in the anterior heart field through a reinforcing autoregulatory loop involving forkhead transcription factors. *Development*. 2004;131:5491–5502.
- Park EJ, Ogden LA, Talbot A, Evans S, Cai CL, Black BL, Frank DU, Moon AM. Required, tissue-specific roles for *Fgf8* in outflow tract formation and remodeling. *Development*. 2006;133:2419–2433.
- Ilgan R, Abu-Issa R, Brown D, Yang YP, Jiao K, Schwartz RJ, Klingensmith J, Meyers EN. *Fgf8* is required for anterior heart field development. *Development*. 2006;133:2435–2445.
- Crossley PH, Martin GR. The mouse *Fgf8* gene encodes a family of polypeptides and is expressed in regions that direct outgrowth and patterning in the developing embryo. *Development*. 1995;121:439–451.
- Sun X, Meyers EN, Lewandoski M, Martin GR. Targeted disruption of *Fgf8* causes failure of cell migration in the gastrulating mouse embryo. *Genes Dev*. 1999;13:1834–1846.
- Frank DU, Fotheringham LK, Brewer JA, Muglia LJ, Tristani-Firouzi M, Capecchi MR, Moon AM. An *Fgf8* mouse mutant phenocopies human 22q11 deletion syndrome. *Development*. 2002;129:4591–4603.
- Abu-Issa R, Smyth G, Smoak I, Yamamura K, Meyers EN. *Fgf8* is required for pharyngeal arch and cardiovascular development in the mouse. *Development*. 2002;129:4613–4625.
- Macatee TL, Hammond BP, Arenkiel BR, Francis L, Frank DU, Moon AM. Ablation of specific expression domains reveals discrete functions of ectoderm- and endoderm-derived FGF8 during cardiovascular and pharyngeal development. *Development*. 2003;130:6361–6374.
- Sekine K, Ohuchi H, Fujiwara M, Yamasaki M, Yoshizawa T, Sato T, Yagishita N, Matsui D, Koga Y, Itoh N, Kato S. *Fgf10* is essential for limb and lung formation. *Nat Genet*. 1999;21:138–141.
- Saga Y, Miyagawa-Tomita S, Takagi A, Kitajima S, Miyazaki J, Inoue T. *MesP1* is expressed in the heart precursor cells and required for the formation of a single heart tube. *Development*. 1999;126:3437–3447.
- Liao J, Aggarwal VS, Nowotschin S, Bondarev A, Lipner S, Morrow BE. Identification of downstream genetic pathways of *Tbx1* in the second heart field. *Dev Biol*. 2008;316:524–537.
- Cai CL, Liang X, Shi Y, Chu PH, Pfaff SL, Chen J, Evans S. *Isl1* identifies a cardiac progenitor population that proliferates prior to differentiation and contributes a majority of cells to the heart. *Dev Cell*. 2003;5:877–889.
- Kelly RG, Papaioannou VE. Visualization of outflow tract development in the absence of *Tbx1* using an *Fgf10* enhancer trap transgene. *Dev Dyn*. 2007;236:811–828.
- Park EJ, Watanabe Y, Smyth G, Miyagawa-Tomita S, Meyers E, Klingensmith J, Camenisch T, Buckingham M, Moon AM. An FGF autocrine loop initiated in second heart field mesoderm regulates morphogenesis at the arterial pole of the heart. *Development*. 2008;135:3599–3610.
- Zhang J, Lin Y, Zhang Y, Lan Y, Lin C, Moon AM, Schwartz RJ, Martin JF, Wang F. *Frs2alpha*-deficiency in cardiac progenitors disrupts a subset of FGF signals required for outflow tract morphogenesis. *Development*. 2008;135:3611–3622.
- Prall OW, Menon MK, Solloway MJ, Watanabe Y, Zaffran S, Bajolle F, Biben C, McBride JJ, Robertson BR, Chaudet H, Stennard FA, Wise N, Schaft D, Wolstein O, Furtado MB, Shiratori H, Chien KR, Hamada H, Black BL, Saga Y, Robertson EJ, Buckingham ME, Harvey RP. An *Nkx2-5/Bmp2/Smad1* negative feedback loop controls heart progenitor specification and proliferation. *Cell*. 2007;128:947–959.
- Hutson MR, Zhang P, Stadt HA, Sato AK, Li YX, Burch J, Creazzo TL, Kirby ML. Cardiac arterial pole alignment is sensitive to FGF8 signaling in the pharynx. *Dev Biol*. 2006;295:486–497.

35. Mesbah K, Harrelson Z, Theveniau-Ruissy M, Papaioannou VE, Kelly RG. Tbx3 is required for outflow tract development. *Circ Res*. 2008;103:743–750.
36. Vincentz JW, McWhirter JR, Murre C, Baldini A, Furuta Y. Fgf15 is required for proper morphogenesis of the mouse cardiac outflow tract. *Genesis*. 2005;41:192–201.
37. Aggarwal VS, Liao J, Bondarev A, Schimmang T, Lewandoski M, Locker J, Shanske A, Campione M, Morrow BE. Dissection of Tbx1 and Fgf interactions in mouse models of 22q11DS suggests functional redundancy. *Hum Mol Genet*. 2006;15:3219–3228.
38. Ornitz DM, Xu J, Colvin JS, McEwen DG, MacArthur CA, Coulier F, Gao G, Goldfarb M. Receptor specificity of the fibroblast growth factor family. *J Biol Chem*. 1996;271:15292–15297.
39. Powers CJ, McLeskey SW, Wellstein A. Fibroblast growth factors, their receptors and signaling. *Endocr Relat Cancer*. 2000;7:165–197.
40. Ohuchi H, Hori Y, Yamasaki M, Harada H, Sekine K, Kato S, Itoh N. FGF10 acts as a major ligand for FGF receptor 2 IIIb in mouse multi-organ development. *Biochem Biophys Res Commun*. 2000;277:643–649.
41. Jerome LA, Papaioannou VE. DiGeorge syndrome phenotype in mice mutant for the T-box gene, Tbx1. *Nat Genet*. 2001;27:286–291.
42. Lindsay EA, Vitelli F, Su H, Morishima M, Huynh T, Pramparo T, Jurecic V, Ogunrinu G, Sutherland HF, Scambler PJ, Bradley A, Baldini A. Tbx1 haploinsufficiency in the DiGeorge syndrome region causes aortic arch defects in mice. *Nature*. 2001;410:97–101.
43. Merscher S, Funke B, Epstein JA, Heyer J, Puech A, Lu MM, Xavier RJ, Demay MB, Russell RG, Factor S, Tokooya K, Jore BS, Lopez M, Pandita RK, Lia M, Carrion D, Xu H, Schorle H, Kobler JB, Scambler P, Wynshaw-Boris A, Skoultschi AI, Morrow BE, Kucherlapati R. TBX1 is responsible for cardiovascular defects in velo-cardio-facial/DiGeorge syndrome. *Cell*. 2001;104:619–629.
44. Garg V, Yamagishi C, Hu T, Kathirya IS, Yamagishi H, Srivastava D. Tbx1, a DiGeorge syndrome candidate gene, is regulated by sonic hedgehog during pharyngeal arch development. *Dev Biol*. 2001;235:62–73.
45. Vitelli F, Morishima M, Taddei I, Lindsay EA, Baldini A. Tbx1 mutation causes multiple cardiovascular defects and disrupts neural crest and cranial nerve migratory pathways. *Hum Mol Genet*. 2002;11:915–922.
46. Zhang Z, Cerrato F, Xu H, Vitelli F, Morishima M, Vincentz J, Furuta Y, Ma L, Martin JF, Baldini A, Lindsay E. Tbx1 expression in pharyngeal epithelia is necessary for pharyngeal arch artery development. *Development*. 2005;132:5307–5315.
47. Vitelli F, Taddei I, Morishima M, Meyers EN, Lindsay EA, Baldini A. A genetic link between Tbx1 and fibroblast growth factor signaling. *Development*. 2002;129:4605–4611.
48. Zhang Z, Huynh T, Baldini A. Mesodermal expression of Tbx1 is necessary and sufficient for pharyngeal arch and cardiac outflow tract development. *Development*. 2006;133:3587–3595.

Novelty and Significance

What Is Known?

- FGF8 signaling from pharyngeal ectoderm is required for correct formation of great arteries.
- FGF8 from second heart field mesoderm is required for arterial pole formation.
- *Fgf10*, like *Fgf8*, is expressed in mesodermal cells of the second heart field.
- *Fgf10* mutants have no detectable great artery or arterial pole defects.

What New Information Does This Article Contribute?

- It reveals a new role of FGF10 in formation of the arterial pole of the heart, when FGF8 is reduced or abolished.
- It reveals a previously unexpected role for mesodermal FGF8 function in great vessel development.

More than 30% of congenital heart defects affect development of the arterial pole of the heart. In the mammalian embryo, cells

that will contribute to this part of the heart derive from mesoderm of the second heart field. Loss of *Fgf8* function in these cells leads to arterial pole defects. *Fgf10* is also expressed in the second heart field, yet *Fgf10* mutants do not have detectable outflow tract or great vessel defects. This may be attributable to compensation by fibroblast growth factor (FGF)8. To address this question, we examined compound mutants and show that arterial pole defects are more severe in the absence of both *Fgf8* and *Fgf10* function in the second heart field. This is also the case for arch arteries that contribute connecting vessels, such as the subclavian and common carotid arteries, revealing for the first time a role for mesodermal FGF8 and FGF10 in vascular development. Our compound mutant analysis also demonstrates that this requirement is highly dosage sensitive, such that progressive reduction in the number of functional alleles of *Fgf8* and *Fgf10* leads to increasingly severe defects. These findings identify *Fgf8* and *Fgf10* as candidate genes for congenital cardiovascular malformations in the human population.

Supplement Material

Online Method

TUNEL assay and Immunohistochemistry

An In Situ Cell Death Detection Kit (Roche) was used for the TUNEL assay. Phospho-Histone H3 antibody (Cell Signaling Technology #9701), Isl1 (DSHB #39.4D5) and AP2 α (DSHB #3B5) antibodies were used for immunohistochemistry.

Online Table I. Number of embryos obtained from $Fgf8^{flox/+};Fgf10^{+/-};MesP1^{Cre/+}$ x $Fgf8^{flox/flox};Fgf10^{+/-}$ crosses.

Genotype	E9.5	E10.5	E15.5/16.5	E18.5	Expected
$Fgf8;Fgf10;Cre$					
$flox/+;+/+$	6 (3.64%)	4 (3.64%)	4 (5.56%)	4 (7.14%)	6.25%
$flox/+;+/-$	28 (16.97%)	12 (10.91%)	7 (9.72%)	6 (10.71%)	12.5%
$flox/+;-/-$	9 (5.45%)	2 (1.82%)	2 (2.78%)	2 (3.57%)	6.25%
$flox/flox;+/+$	11 (6.67%)	12 (10.91%)	5 (6.94%)	7 (12.5%)	6.25%
$flox/flox;+/-$	18 (10.91%)	15 (13.64%)	7 (9.72%)	6 (10.71%)	12.5%
$flox/flox;-/-$	14 (8.48%)	10 (9.09%)	3 (4.17%)	2 (3.57%)	6.25%
Total number	165	110	72	56	

Online Figure legend

Online Figure I. Apoptosis and proliferation in $Fgf8;Fgf10$ compound mutants. (A-F) TUNEL assay was performed at E9.5. (A,C) Control $Fgf8^{flox/+};Fgf10^{+/-}$ embryo shows some cell death in the pharyngeal endoderm (PE) (arrow heads). (B,D) This is increased in the PE and OFT of the $Fgf8^{flox/flox};Fgf10^{-/-}$ mutant. (A,B) The number of phospho-histone H3 (PHH3) positive cells (arrows) is also less in $Fgf8^{flox/flox};Fgf10^{-/-}$ mutants (B) compared to control $Fgf8^{flox/+};Fgf10^{+/-}$ embryos (A). (E,F) Transverse sections at the level of developing fourth PAA in E9.5 embryos show apoptosis in the AP2 α -positive cells on the right side of the $Fgf8^{flox/flox};Fgf10^{+/-}$ mutant (E), but not in control $Fgf8^{flox/+};Fgf10^{+/-}$ embryos (F). Asterisks indicate the dorsal aorta.

Online Figure I

